

GT2011-46057

INTERACTIONS OF SEPARATION BUBBLE WITH ONCOMING WAKES BY LES

S. Sarkar

Indian Institute of Technology Kanpur
Kanpur, UP, India

Jasim Sadique

Indian Institute of Technology Kanpur
Kanpur, UP, India

ABSTRACT

The unsteady flow physics and heat transfer characteristics due to interactions of periodic passing wakes with a separated boundary layer are studied with the help of Large-eddy simulations (LES). A flat plate with a semicircular leading edge is employed to obtain the separated boundary layer. Wake data extracted from precursor LES of flow past a cylinder are used to replicate a moving bar that generates wakes in front of a cascade (in this case an infinite row of flat plates). This setup is a simplified representation of the rotor-stator interaction in turbomachinery. With a uniform inlet, the laminar boundary layer separates near the leading edge, undergoes transition due to amplification of the disturbances, becomes turbulent and finally reattaches forming a bubble. In the presence of oncoming wakes, the characteristics of the separated layer have changed and the impinging wakes are found to be the mechanism affecting the reattachment. Phase averaged results illustrate the periodic behaviour of both flow and heat transfer. Large undulations in the phase-averaged skin friction and Nusselt number distributions can be attributed to the excitation of separated shear layer by convective wakes forming coherent vortices, which are being shed and convect downstream. This interaction also breaks the bubble into multiple bubbles. Further, the transition of the shear layer during the wake-induced path is governed by a mechanism that involves the convection of these vortices followed by increased fluctuations.

Keywords: Separation Bubble, transition, periodic wake, LES, IB method.

INTRODUCTION

The flow in turbomachinery is highly unsteady due to the wakes shed by upstream rows of blades interacting with the boundary layer forming on the downstream blades. Wake passing not only influences the boundary layer transition, it causes periodic fluctuations of pressure and formation of coherent vortices [1-4]. The presence of wakes can also lead to a reduction in the separation bubble length. The boundary layer transition is brought about directly by the disturbances of convective wakes. The interaction of wake with the separated layer has been studied extensively using linear cascades and wake generators, both experimentally and numerically. Meyer [5] described the wake kinematics by replacing each wake by a perturbation jet ("negative jet") on a uniform flow. The wake-affected velocity profiles of the boundary layer on the leading edge of a blunt test model were measured in Ref. [6]. The effect of flow coefficient ($C_\theta = U_o/U_b$) on a flat plate with elliptical leading edge subjected to periodic passing wakes was elucidated by Ref. [7]. Reference [8] carried out a numerical simulation on a boundary layer developing on a flat plate, affected by passing wakes. They observed a receptivity phase where the wake causes enhanced disturbances in the boundary layer. They also studied the evolution of turbulent spots and used phase averaging to characterize the flow. Reference [9] used hot wire measurements to study the wake-separation bubble interaction on a flat plate with a semicircular leading edge at a high Reynolds number (based on inlet velocity and leading edge diameter) of 6.67×10^4 . They observed the formation of turbulent spots followed by a calmed region behind the wake, which acted to suppress the separation. The characteristics of wake passing on the suction side of a low-

pressure (LP) turbine blade has been studied experimentally [10], and numerically by LES [11] and DNS [12]. They all confirmed the formation of the coherent vortices by the rollup of the shear layer via Kelvin-Helmholtz (KH) mechanism. These vortices are identified as the source of pressure fluctuations on the suction surface. A flow and heat transfer analysis in a turbine cascade in the presence of incoming wakes using DNS was conducted by Ref. [13], where the incoming wakes were generated using a moving row of cylinders. Reference [14] performed a study in which the Reynolds number and the wake passing frequency were varied and compared the results with steady flow conditions. The C_p distribution displayed increased loading with a shorter separated region for the higher Reynolds number, indicating the separation bubble had been reduced in height and length. Boundary layer measurements confirmed these observations and revealed the separation bubble contracting and expanding as the wake passed. The small-scale fluctuations carried by the convective wake influences the transition to turbulence of the highly diffusive boundary layer on the suction surface [2,4]. Thus, the unsteady flow on the suction surface is dependent on the turbulence intensity and the length scale of passing wakes. The physical mechanism of transition, of an inflectional boundary layer over the suction surface of a highly cambered low pressure (LP) turbine blade under the influence of periodically passing wakes has been studied by Ref. [15,16].

We aim to capture the physics of wake bubble interactions at a relatively low Reynolds number of 3450 (based on inlet flow velocity and leading edge diameter). For simplicity, the study is carried out on a flat plate with a semicircular leading edge (here the separation is induced by the geometry and not adverse pressure gradients). It appears that there is relatively lesser number of studies at this range of Reynolds numbers, which is of significance in the case of low speed operation of turbines. Under these conditions, there may be a relatively large bubble formed due to flow separation near the leading edge or on the rear half of the suction surface. This may change flow characteristics as compared to those of high Reynolds number flows. LES is used for its ability to provide the detailed spatial and temporal information regarding a wide range of turbulence scales, which is essential to gain a better insight in to the flow physics.

NOMENCLATURE

C_f	skin friction coefficient
D	Leading-edge diameter
D_{cyl}	Wake generating cylinder diameter
f	Bar passing frequency
l	Bubble length
Nu	Nusselt number
Pr	Prandtl number
Re	Reynolds number based on D

Re_{cyl}	Reynolds number based on D_{cyl}
St	Stanton Number
T	Temperature
T'	r.m.s. temperature fluctuations
T_{in}	Inlet Temperature
T_b	Body wall temperature
t	time
t_p	time period of wake passing
U	velocity component in x-direction
U_0	inlet velocity
u', v', w'	r.m.s. velocity fluctuations
$\langle u'T' \rangle, \langle v'T' \rangle, \langle w'T' \rangle$	Turbulent heat transfer quantities
x, y, z	Cartesian coordinates
Δt	time step for main simulation
$\Delta x^+, \Delta y^+, \Delta z^+$	grid spacing in terms of wall units

COMPUTATIONAL DETAILS

The three-dimensional (3-D) unsteady filtered Navier-Stokes equations are solved for Newtonian incompressible flow in the Cartesian coordinate system along with energy equation. A dynamic subgrid-scale model proposed by Germano [17] and modified by Lilly[18] is used to model the SGS stress tensor and temperature flux, which represent the effect of subgrid motion on the resolved field of LES. Here, the model coefficient is dynamically calculated instead of input a priori. To resolve the leading edge in Cartesian geometry, the Immersed Boundary method is used here to apply the boundary conditions where the geometry is non-conformal to the grid.

The equations are discretized in space using a second order symmetry preserving central difference scheme, which are widely used in LES for their non-dissipative character [19,20]. The time advancement is explicit using the second-order Adams-Bashforth scheme [21] except for the pressure term, which is solved by a standard projection method. The pressure equation is discrete Fourier transformed in one dimension (in which the flow can be considered homogeneous) and is solved by the BI-CG algorithm in the other two directions [22]. For applying the boundary conditions, IB technique is used following Ref. [23], which belongs to the class of 'direct forcing method'. The velocity and temperature field near the boundary of the body is modified at each step in such a way that the no-slip boundary condition and the constant temperature wall are satisfied. This is done using an interpolation technique, which is equivalent to including a body force F_i in the momentum and F_T in the energy equations. In the present simulation the quadratic unidirectional interpolation technique [24,25] is used. The solver used in the present

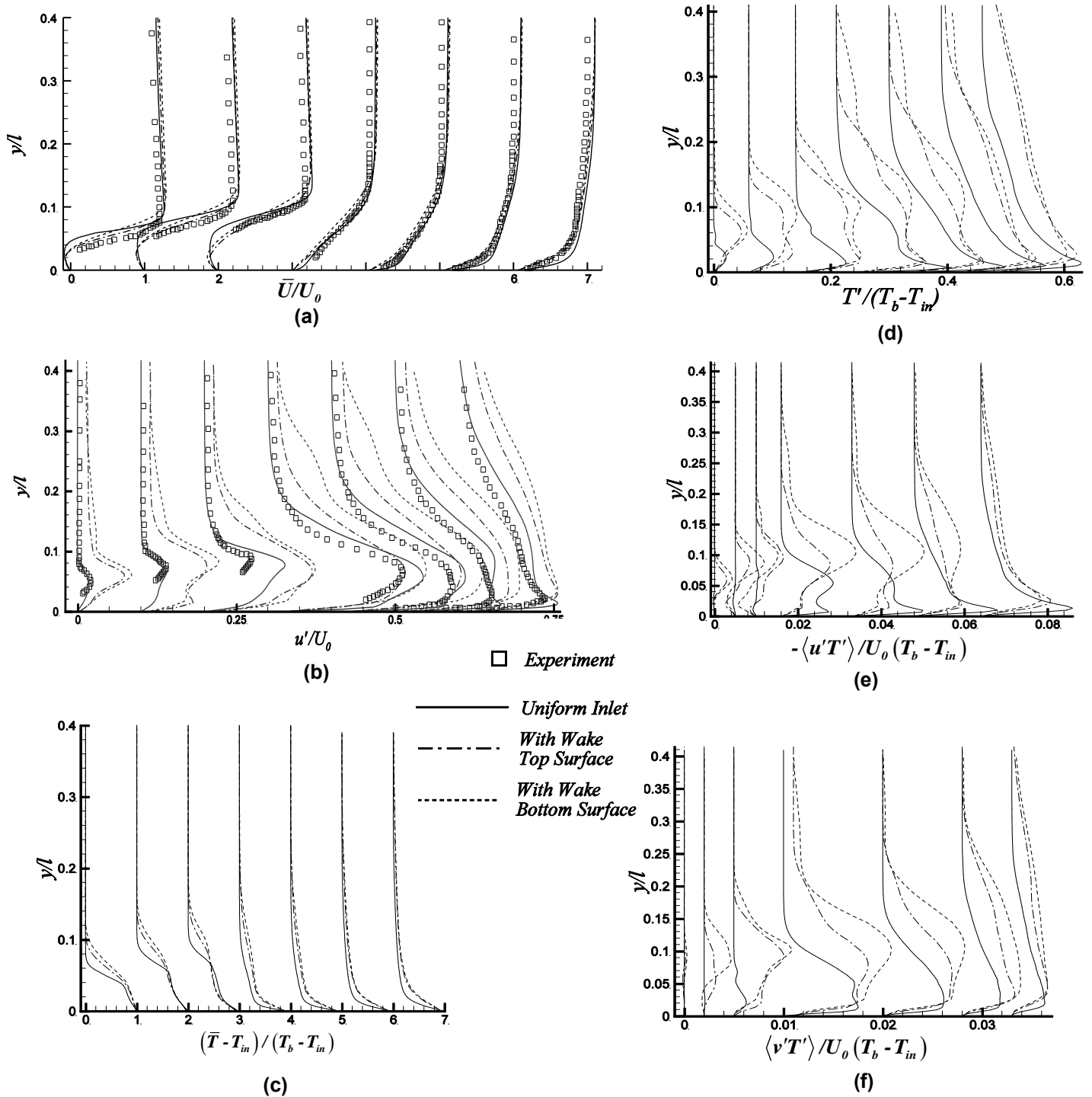


Figure 2 (a) Mean axial velocity, (b) r.m.s. stream wise velocity fluctuation u' (c) Mean Temperature profile, (d) r.m.s. temperature fluctuations, (e) streamwise turbulent heat flux $-\langle u'T' \rangle$ (f) wall normal heat flux $\langle v'T' \rangle$ computed at seven stream wise locations measured from the blend point at $x/l=0.22, 0.44, 0.66, 1.09, 1.27, 1.64, 2.55$.

The r.m.s. streamwise velocity fluctuations (u') with and without wakes are compared with experimental results as depicted in Fig. 2b. The case with uniform inlet matches well with the results of [28], although there exists some discrepancies near the location $x/l=0.66$. The agreement with the experiment is much better after the reattachment and the boundary layer approaches to a canonical layer. With oncoming wakes, the values of u' are more in the separated shear layer particularly in the outer region of the flow. This is attributed to the enhanced receptivity to perturbations of the separated shear layer and its excitation by passing wakes. Further, the coherent vortices appear because of rollup of separated layer, which enhances turbulence in the outer layer. After reattachment, the discrepancy reduces as we move downstream. There is also a difference in values between the top and bottom surfaces- the amplitude seems to be more on the lower half as compared to the upper half. This is due to the wake kinematics and associated small-scale interactions of wake fluid with the separated shear layer, which is different on both surfaces. However, here there will be no effect of pressure gradients as seen in Refs. 15 and 29. On the lower half the wake impinges directly on the surface and counter-clockwise vortices of the wake pushes the shear layer, whereas, for the top surfaces wake vortices have a tendency to lift-off the shear layer being of opposite signs, which will be discussed in further detail later. This results in increase in the r.m.s. value of fluctuation components on the bottom surface.

The mean temperature profiles are plotted in Fig 2c and r.m.s. value of its fluctuation (T') in Fig 2d. For the case of flow with a uniform inlet, the temperature fluctuations exhibits a more complex behaviour unlike the velocity fluctuations with a maximum near the wall and a local maximum in the outer shear layer. This double peak behaviour was also reported in a DNS of a separated boundary layer on a flat surface [30]. The high near wall temperature fluctuations indicates a preponderance of dissipation. With wake passing, a significant enhancement of temperature fluctuations is observed away from the wall and may be related to the formation and convection of coherent vortices. The location of the outer peak of T' shifts away from the wall along the edge of the separated layer. A similar effect is also seen in the turbulent heat fluxes $\langle u'T' \rangle$, $\langle v'T' \rangle$ (Fig 2e and f). In the outer region, the values of heat fluxes are significantly higher for the bottom surface than those of the top surface. After reattachment the near wall heat fluxes predominates illustrating an equilibrium layer.

The C_f distribution at the top and bottom surfaces is given in Fig. 3 along with the C_f for the case with uniform velocity inlet. The separation and reattachment points of the mean flow are located by the zero crossing of the skin friction plots. The initial flat portion after the separation point corresponds to the dead air region of the bubble, whereas, the reverse flow vortex region is associated with a much larger negative skin friction. This is similar to the flow structure of a short laminar separation bubble [31]. The separation bubble length obtained from the present LES with uniform flow is around 4.1D, which is over predicted due to difference in inlet turbulence level and

blockage-ratio. With wake, remarkable difference is observed in the distribution over the two surfaces, and the time-averaged bubble length obtained is around 2.04D for the top surface, whereas, it is 1.63D for the bottom surface. The reduction in bubble length is due to the increased perturbation caused by the wake impingement, resulting in faster transition to turbulence, which is illustrated later.

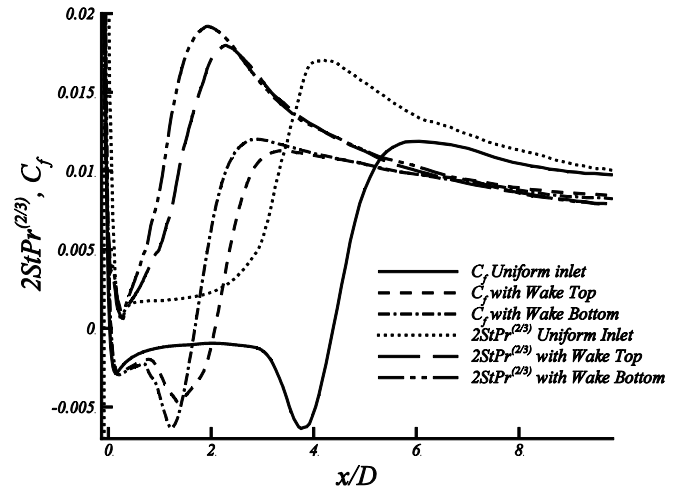
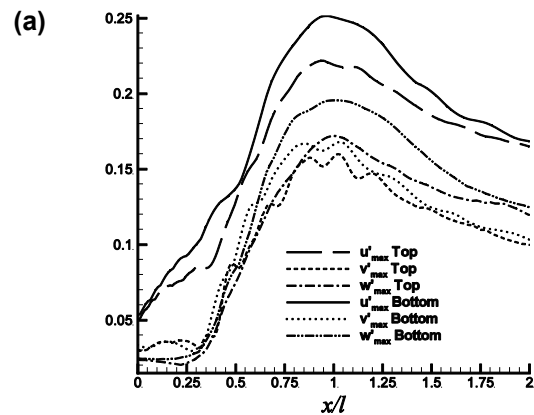


Figure 3 Time-averaged coefficient of friction (C_f) along with Stanton number (St_x)

To illustrate the evolution of heat transfer in the separated region, the distribution of Stanton number numbers over the top and bottom surfaces, along with the values for the case with uniform velocity inlet, are superimposed on the C_f distribution (Fig. 3). A factor of $2Pr^{(2/3)}$ is used for flow and heat transfer analogy, given by Colburn [32] based on experimental data for both laminar and turbulent flows, which has been widely used. The Stanton numbers, even with the wake, have a similar trend as that reported in Ref. [30]. The Stanton number becomes maximum at the point where the C_f is minimum, which corresponds to the breakdown of shear layer. As downstream is approached $2StPr^{(2/3)}$ slowly drops down and approaches the value of C_f illustrating an equilibrium boundary layer.



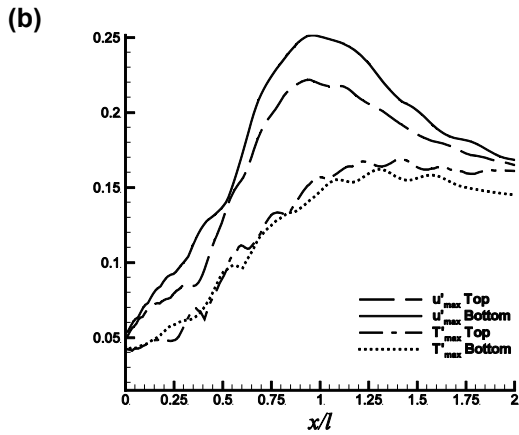


Figure 4. (a) Profiles of maximum r.m.s values of velocity fluctuations and (b) Profiles of maximum r.m.s values of temperature fluctuations superimposed with streamwise velocity fluctuations for flow with passing wakes

The growth of disturbances and the development of three-dimensional motion can be illustrated by the evolution of velocity fluctuations. Figure 4a shows the peak values of velocity fluctuations (r.m.s.) in the streamwise, wall normal and span-wise directions for both the top and bottom surfaces, starting from the blend point. Even at the onset of separation the fluctuations have non-zero values, followed by an increase of u' with relatively slower rate up to $x/l = 0.35$ and then it increases rapidly in the second half of the bubble for the upper surface, while for the lower surface the increase of u' occurs at the same rate from the beginning. However the trend is a bit different for v' and w' . They start growing from $x/l = 0.3$, increases rapidly in the second half of the bubble lagging behind u' . The peak values reach a maximum around the mean reattachment point and then tend to drop slowly illustrating the end of transition. The relatively large value of w' shows the presence of significant three-dimensional motions which causes the flow to breakdown to turbulence. The shear layer is highly anisotropic with a very high value for the streamwise component of velocity fluctuations. The peak values are more in the bottom half as compared to the top half especially near reattachment. This difference reduces as the boundary layer relaxes downstream. The value of u' approaches around 16% at $x/l = 2.5$, while v' and w' show slower relaxation and drop to a value of around 5% and 7% respectively at $x/l = 4.0$. The maximum r.m.s. value of temperature fluctuations are shown in Fig 4b and compared with u' . The temperature fluctuations follow the velocity fluctuations in the separated layer, but with a relatively slower rate and lags the velocity fluctuations, reaching a maximum around 17% near $x/l = 1.25$. However, there is not much reduction in the fluctuations after reattachment and it stays around 16% in the downstream locations.

Instantaneous Flow Field and Thermal characteristics

The contours of streamwise velocity and temperature at two instances are depicted in Fig 5 to visualize the internal growth mechanism of the shear layer and three-dimensional

flow structures due to excitation by passing wakes. At $t/t_p=0.3$, when the wake is ahead of the shear layer, the instability of separated layer occurs because of enhanced receptivity to perturbations. For the velocity (Fig 5a) in the xy plane (side view), the darkest gray-scale in the velocity contours represent the separation region. The side view also illustrates thickening of shear layer over the bubble and its rollup, forming large-scale vortices via KH instability, which may retain their structures far downstream. In the xz plane (top view), for a wall-normal location of $y/D = 0.04$, three-dimensional motions sets in near $x/D = 0.3$ and starts growing. The formation of longitudinal streaks, the characteristics of a transitional layer, appears near $x/D=1$, breaking down near the reattachment. However there are some differences in flow structure for lower and upper surface mainly due to differences in the length of separation bubble. The temperature contours (Fig 5b) closely follow the velocity, although it elucidates the three-dimensional structures better. It clearly explains the appearance of three-dimensional motions at $x/D = 0.3$, followed by longitudinal streaks that undergo elongation and finally breakdown near reattachment. The appearance of streaks are visible even after reattachment illustrating a slow relaxation to a canonical layer after $x/D = 4.0$. The formation of coherent vortices due to rollup of shear layer and their convection retaining their identity far downstream are well resolved here [34,35].

The wake affected boundary layer is illustrated by velocity contours for the instant $t/t_p=0.6$. It is interesting to note that as the wakes pass over the bubble the flow structure changes. From the velocity contours (Fig. 5c) in the xy plane, we see that the negative jet effect of the wake deforms the shear layer resulting in multiple vortices that convect downstream, changing the instantaneous separation point in the process. The structures are similar to those of wake passing over an LP turbine [1,13,15,29]. A trail of three prominent large-scale vortices is formed. From the xz plane we find that the 3-D motions set in very early. It appears that the large-scale vortices in the lower surface are of relatively smaller dimension as compared to those on the upper surface: attributable to difference in wake kinematics. The temperature contours (Fig. 5d) also show the excitation of the shear layer, its stretching, formation of large-scale vortices and their breakdown in a similar manner to the flow when wake is ahead of the bubble. The difference in flow structure between the upper and lower surface is more pronounced here with the streaks on the lower surface having less spacing between them as compared to those on the upper surface. In the downstream, the flow is associated with large-scale coherent vortices apart from adequate small-scale eddies. The significant differences between the events of the two instances are that the passing wakes cause formation of multiple vortices and transition of shear layer occurs at a faster rate. It is interesting to note that the mechanism of transition remains similar during wake induced path, i.e. the inviscid instability of separated layer by external excitations forming vortices which finally breakdown near reattachment.

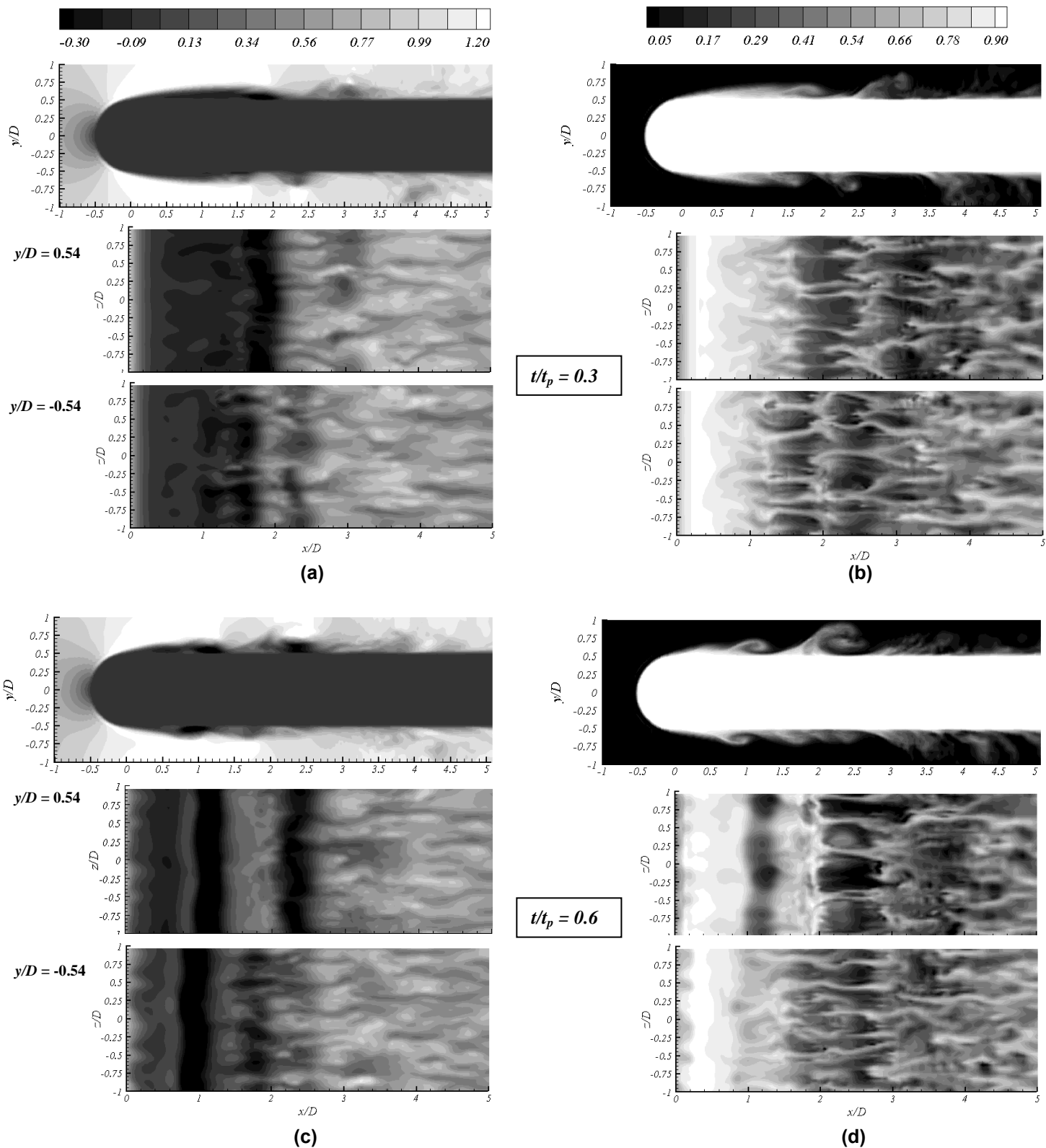


Figure 5. Contours of instantaneous (a) streamwise velocity and (b) temperature in the xy plane (at midspan) and the xz plane (at $0.04D$ from both top and bottom walls) at $t/t_p=0.3$ and (c) and (d) are at $t/t_p=0.6$

Spectra

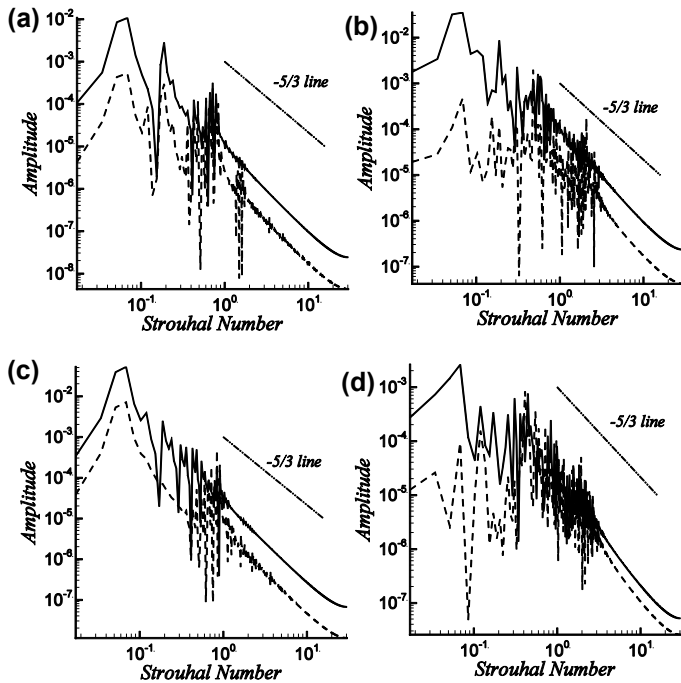


Figure 6. Spectra of streamwise velocity and temperature fluctuations at two stations at $x/l = 0.35$, and 1.25 and at $y/l = 0.04$ from the wall. (a) and (b) are for the upper surface while (c) and (d) are for the lower surface. Solid line is u' and dashed line T'

LES data stored at two different streamwise locations $x/l = 0.35, 1.25$ along a line $y/l = 0.04$ from the wall, in the mid-span were processed to get the velocity and temperature spectra of both top and bottom surfaces. The results presented below in Fig. 6 correspond to samples at each point taken over seven wake-passing periods. A peak at all these locations is present at $0.06U_0/D$, which corresponds to the wake passing frequency. The results presented earlier illustrate that as the wake passes over the separated layer, large-scale vortices are formed and shed downstream. At $x/l = 0.35$ the power spectra of u' and T' indicate that the vortex shedding is not periodic with a single frequency, rather shedding process seems to happen with a wide range of frequency roughly from $0.4U_0/D - 0.9U_0/D$ at the top surface. In the bottom surface at the same location shedding appears to occur in a wider range of $0.4U_0/D - 2.0U_0/D$. Even after reattachment at $x/l = 1.25$, the presence of large-scale vortices is apparent along with more energetic high frequency harmonics. These are attributed to the breakdown of coherent vortices to small-scale energetic eddies downstream. The slope of the resolved inertial range appears to follow the $-5/3$ power law correlation between the energy and frequency. Thus, the mesh used in the present LES appears good to resolve wake boundary layer interactions.

Phase Averaged Results

Phase averaging is used to garner greater understanding of the flow physics at different wake positions with respect to the

body. The predominant time scale present in the problem is the wake passing cycle, which is divided into 25 uniform time brackets for the purpose of calculating the phase averages.

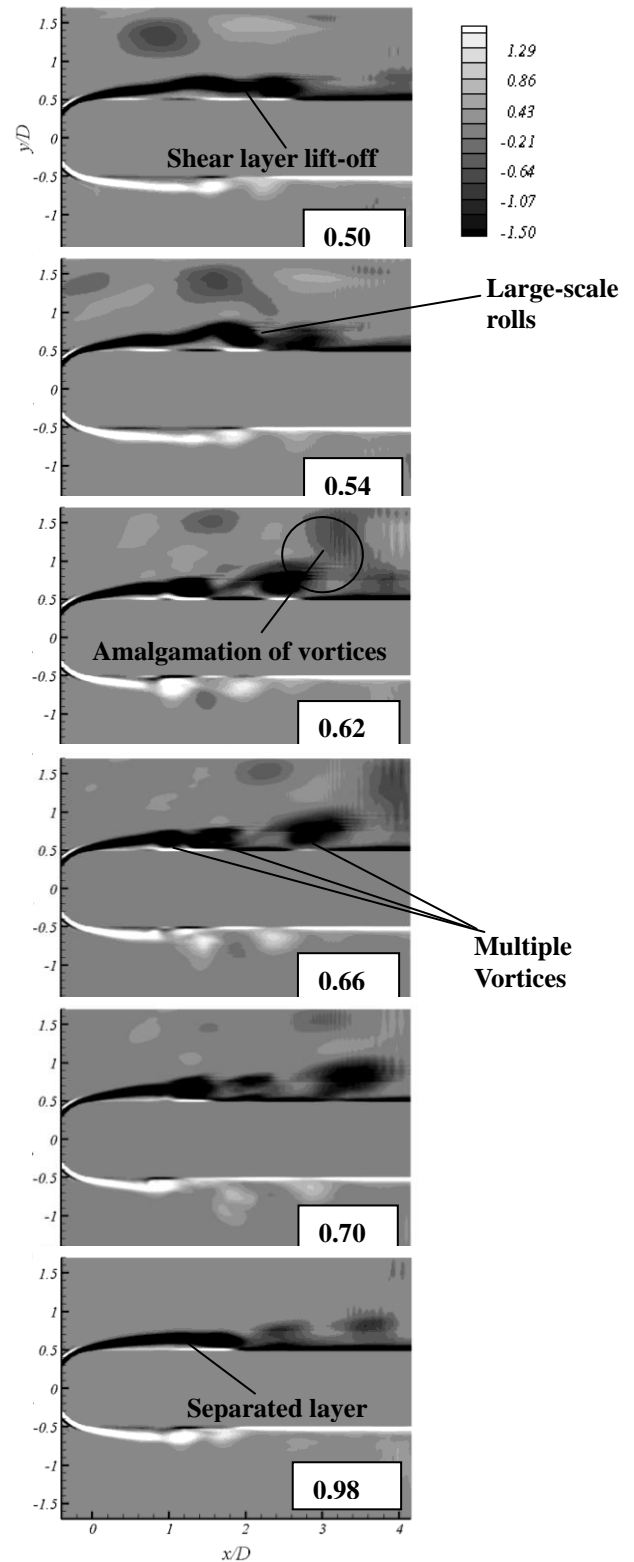


Figure 7. Contours of phase-averaged vorticity illustrating wake boundary layer interactions

Figure 7 depicts the contours of phase-averaged streamwise component of vorticity to illustrate the interactions of wake and separated shear layer. The interactions of wake on a boundary layer has been explained previously by the "negative jet" effect that impinge on the shear layer and develops coherent vortices influencing boundary layer characteristics [5,11]. In the present study, the mutual interactions of wake and shear layer vortices is explained in terms of vortex dynamics concentrating on the upper surface. The upstream translating cylinder sheds Kármán vortices that convect along with the flow. These vortices after being segmented at the leading edge and because of local acceleration undergo a rotation and the positive vortex will approach the shear layer, which has a negative vorticity. This causes the shear layer to lift-off being of opposite sign and to undergo elongation. This results in rollup because of inviscid instability, which creates a large-scale vortex. The convection of these vortices appear slower than that of the wake. As time progresses, we observe amalgamation of rolls with the negative wake vortices producing a very significant large roll that convects downstream and which retains its identity in the far downstream. As the wake passes over the separation region it creates a train of three prominent coherent vortices, which convects downstream and eventually break down to turbulence. After wake passing, the boundary layer relaxes as the influence of wakes subsides and the flow characteristics become similar to separated flow induced by the leading edge. On the lower surface, a similar flow dynamics is observed with the stretching of the shear layer, formation of large-scale vortices and their convection downstream. However, the lift-off of shear layer is not as severe as that of upper surface. This mechanism is quite similar to what is observed in turbine blades [1,10], although effect of pressure gradients is absent here. This might suggest that the mutual interactions between wake and shear layer vortices is the driving factor in exciting the boundary layer rather than the effect of pressure gradients.

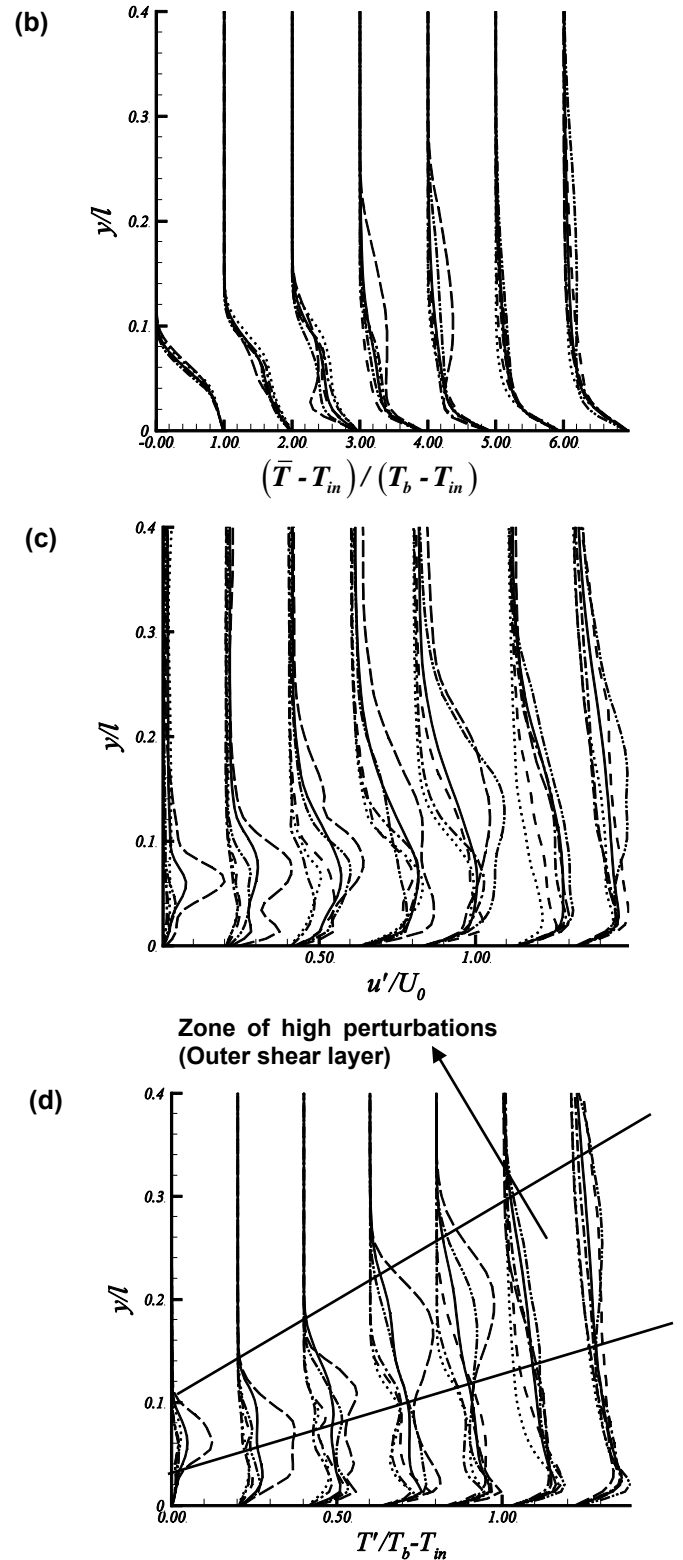


Figure 8. Profiles at different phases of (a) axial velocity, (b) Mean Temperature profile, (c) r.m.s. u' , (d) r.m.s. T' on top surface along with time averaged profiles at $x/l=0.22, 0.44, 0.66, 1.09, 1.27, 1.64, 2.55$ from the blend point

The phase-averaged profiles for streamwise velocity, temperature, their fluctuations (r.m.s) and turbulent heat fluxes at seven streamwise locations for the top surface are shown in

Fig 8. At the phases t/t_p 0.02 and 0.22, the wakes are well ahead of the bubble, while at 0.62 the wake causes rollup of the shear layer. At t/t_p 0.82, the wake has just passed the bubble and the rolls are being convected away. Along with the phase-averages, time-averaged profiles are also superimposed to understand the effect of coherent vortices. For the streamwise velocity and temperature (Fig 8a,b), there is not much variation in the different phases up to $x/l = 0.44$. The change is very prominent in the second half of the bubble because of formation of KH rolls. However, both velocity and temperature fluctuations (Fig 8c,d) show significant increase in the wake-affected path from the beginning, particularly in the outer shear layer. This is due to the convection of vortices, whose path can be identified from the profiles by following the peak regions. As the downstream is approached, high fluctuations are predominant near the wall for all phases, becoming similar to time-averaged profile illustrating the relaxation of boundary layer. A similar behaviour is observed for the turbulent heat fluxes with local concentration in the outer region. This is attributed to the convection of large-scale eddies, illustrating temporally and spatially varying concentration of vorticity and turbulent stresses, which are significantly greater in the outer shear layer.

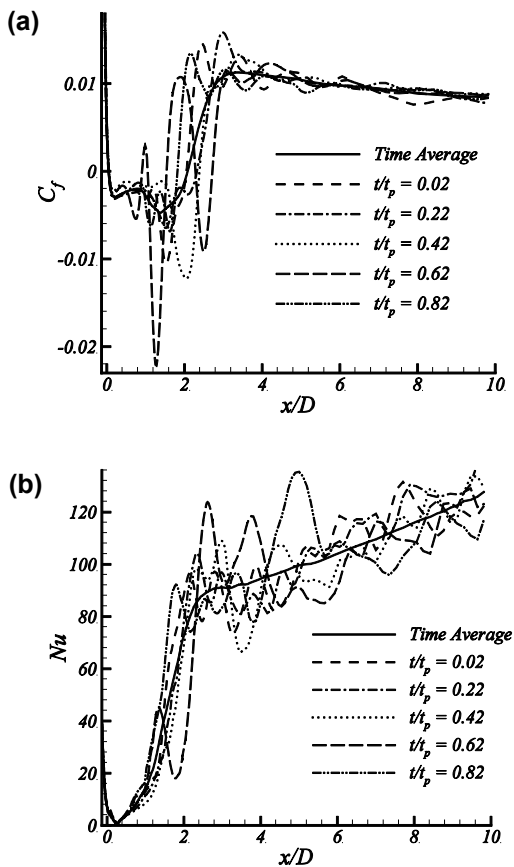


Figure 9. Phase averaged (a) C_f and (b) Nu distribution at the top surface superimposed with time-averaged distribution

The Phase averaged skin friction and Nusselt number distribution are shown (Fig 9a,b) along with time-averaged

values. Among the phases shown the deviations from the mean distributions are most prominent for the phase at $t/t_p = 0.62$ which is in the wake affected path. The skin friction distribution shows the large undulations in the flow and the presence of multiple bubbles. This is attributed to the excitation of separated shear layer by convective wakes forming coherent vortices. These also cause a variation in the reattachment point at different phases. The undulations are maximum in the separated layer and reduce as we move downstream elucidating the breakdown to more energetic eddies. The heat transfer characteristics illustrates the same trend, however, the oscillations in the Nusselt number distribution is felt far downstream. Thus the transition over the separated layer is governed by a mechanism that involves the formation of these vortices followed by concentration of local fluctuations. There are multiple peaks indicating numbers of large-scale vortices changing the instantaneous reattachment region and thus transition length. A similar observation was found for the flow over an LP turbine blade with periodic wake passing [15].

CONCLUSIONS

The flow and heat transfer characteristics of the separated flow under influence of periodic passing wake are analysed through LES. Results presented are validated against the available experimental data on a flat plate having a semi-circular leading edge with a uniform inlet. The time-averaged results illustrate that with oncoming wakes both temperature and velocity fluctuations increase from the onset of separation. However, growth is very high in the second half of the bubble and the turbulent activities are significant in the outer layer. The separated region and transition length are reduced compared to flow without wakes. The separation length is smaller and amplitude of fluctuations is higher on the bottom surface as compared to the top surface attributable to the difference in wake kinematics.

The instantaneous results illustrate the excitation of shear layer by passing wakes and formation of three-dimensional flow structures. When the wake is ahead of the shear layer, the instability of separated layer occurs because of enhanced receptivity to perturbations forming large-scale vortices, which may retain their identity far downstream. The temperature contours closely follow the velocity, although it elucidates the three-dimensional structures better. The appearance of streaks is visible even after reattachment illustrating a slow relaxation to a canonical layer. It is interesting to note that the mechanism of transition remains similar during wake induced path, i.e. the inviscid instability of separated layer by external excitations forming vortices, which finally breakdown near reattachment. However, transition length changes appreciably.

Phase-averaged flow visualization is used to illustrate the vortex dynamics behind the wake and boundary layer interactions. For the top surface wake vortices have a tendency to lift-off the shear layer being of opposite signs, whereas, on the lower half the wake impinges directly on the surface and counter-clockwise vortices of the wake pushes the shear layer. It has been observed that there will be stretching of shear

layer resulting in multiple vortices that convect downstream amalgamating with wake fluid and eventually breaking down to turbulent flow. We find that the rollup vortices have a very high influence on the generation of turbulence apart from causing regions of concentrated stress and turbulent heat fluxes. This is similar to what is observed in a highly cambered low-pressure turbine blade subjected to periodic convective wakes, where there was substantial effect of pressure gradient. Thus, the mutual interactions between wake and shear layer vortices appears to be primarily responsible in exciting the separated boundary layer.

ACKNOWLEDGMENTS

The authors would like to acknowledge the financial grants from Propulsion Panel, Aeronautics R&D Board, Govt. of India for carrying out the present work.

REFERENCES

- [1] Sarkar, S., 2008, "Identification of flow structures on a LP turbine blade due to periodic passing wakes," *ASME J. Fluids Eng.*, **130**, 061103.
- [2] Sarkar, S., 2009, "Influence of wake structure on unsteady flow in an LP turbine blade passage," *ASME J. Turbomach.*, **131**, 041016.
- [3] Hodson HP, Howell RJ, 2005, "The role of transition in high-lift low-pressure turbines for aeroengines," *Prog. Aerospace Sciences*, **4**, pp419-454.
- [4] Wissink, J. G., Rodi, W., and Hodson, H., 2006, "Influence of Disturbances Carried by Periodically Incoming Wakes on the Separating Flow Around a Turbine Blade," *Int. J. Heat Fluid Flow*, **27**, pp. 721–729.
- [5] Meyer, R. X., 1958, "The Effects of Wakes on the Transient Pressure and Velocity Distributions in Turbomachines," *ASME J. Basic Eng.*, **80**, pp. 1544–1552.
- [6] Paxson, D.E. and Mayle, R.E., 1991, "Laminar Boundary Layer Interaction with an Unsteady Passing Wake," *ASME J. Turbomach.*, **113**, pp. 419-427.
- [7] Holland, R. M. and Evans, R.L., 1996, "The Effects of Periodic Wake Structures on Turbulent Boundary Layers," *J. Fluids Structures*, **10**, pp.269-280.
- [8] Wu, X., Jacobs, R. G., Hunt, J. R. C., and Durbin, P. A., 1999, "Simulation of Boundary Layer Transition Induced by Periodically Passing Wakes," *J. Fluid Mech.*, **398**, pp. 109–153.
- [9] Funazaki, K., Kato, Y., 2002, "Studies in a Blade Leading Edge Separation Bubble Affected by Periodic Wakes: Its Transitional Behaviour and Boundary Layer Loss Reduction," *ASME Paper No. GT-2002-30221*.
- [10] Stieger, R., Hollis, D., and Hodson, H., 2003, "Unsteady Surface Pressures Due to Wake Induced Transition in Laminar Separation Bubble on a LP Turbine Cascade," *ASME Paper No. GT2003–38303*.
- [11] Wissink, J. G., 2003, "DNS of Separating, Low Reynolds Number Flow in a Turbine Cascade With Incoming Wakes," *Int. J. Heat Fluid Flow*, **24**, pp.626–635.
- [12] Sarkar, S., Voke, P., 2006, "Large-eddy simulation of unsteady surface pressure on a LP turbine blade due to interactions of passing wakes and inflexional boundary layer," *ASME J. Turbomech.*, **128**, pp. 221-231.
- [13] Wissink, J.G., Rodi W., 2006, "Direct Numerical Simulation of flow and heat transfer analysis in a turbine cascade in the presence of incoming wakes", *J. Fluid Mech.*, **569**, pp 209-247.
- [14] Schobeiri, M. T., Öztürk, B., and Ashpis, D. E., 2007, "Effect of Reynolds Number and Periodic Unsteady Wake Flow Condition on Boundary Layer Development, Separation, and Intermittency Behavior Along the Suction Surface of a Low Pressure Turbine Blade," *ASME J. Turbomach.*, **129**, pp. 92-107.
- [15] Sarkar, S., 2007, "The effects of passing wakes on a separating boundary layer along a low-pressure turbine blade through large-eddy simulation," *Proc. Inst. Mech. Eng., Part A*, **221**, pp. 551-564.
- [16] Sarkar, S., 2007, "Large-eddy simulation of wake convection and unsteady flow in a LP turbine blade passage," *Prog. Comput. Fluid Dyn.*, **7**, pp. 387-403.
- [17] Germano, M., Piomelli, U., Moin, P., Cabot, W. H., 1991, "A dynamic subgrid-scale eddy viscosity model," *Phys. Fluids A*, **3**, pp. 1760-1765.
- [18] Lilly, D.K., 1991, "A proposed modification of the Germano subgrid-scale closure method," *Phys. Fluids A*, **4**, pp. 633-635.
- [19] Mittal, R., and Moin, P., 1997, "Suitability of Upwind-Biased Finite-Difference Schemes for Large-Eddy Simulation of Turbulent Flows," *AIAA J.*, **35**, pp. 1415–1417.
- [20] Morinishi, Y., Lund, T. S., Vasilyev, O. V., and Moin, P., 1998, "Fully Conservative Higher Order Finite Difference Schemes for Incompressible Flow," *J. Comput. Phys.*, **143**, pp. 90–124.
- [21] Chorin, A. J., 1968, "Numerical solution of the Navier–Stokes equations," *Math. Comp.*, **22**, pp. 745–762.
- [22] Zhang, S. L., 1997, "GPBI-CG: Generalized product-type methods based on Bi-CG for solving nonsymmetric linear systems," *SIAM J. Scientific Comput.*, **18**, pp 537-551.

- [23] Fadlun, E. A., Verzicco, R., Orlandi, P. and Mohd.-Yusof, J., 2000, "Combined immersed boundary finite difference methods for three dimensional complex flow simulations," *J. Comput. Phys.*, **161**, pp. 35-60.
- [24] Muldoon, F. and Acharya, S., 2005, "Mass conservation in immersed boundary method, Proceeds. FEDSM 2005," FEDSM-77301, pp. 1-9.
- [25] S. Sarkar and Sudipto Sarkar, 2009, "Large-Eddy Simulation of Wake and Boundary Layer Interactions Behind a Circular Cylinder," *ASME J. Fluids Engineering*, **131**, 091201.
- [26] Orlanski, I., 1976, "Simple boundary condition for unbounded hyperbolic flows," *J. Comput. Phys.*, **21**, pp. 251-269.
- [27] Yang, Z.Y. & Voke, P.R., 2001, "Large eddy simulation of boundary layer separation and transition at change of surface curvature," *J. Fluid Mech.*, **439**, pp. 305-333.
- [28] Coupland, J., Brierley, D., 1996, "Transition in turbomachinery flows," Final Report, BRITE/EURAM Project AERO-CT92-0050.
- [29] Wu, X., and Durbin, P. A., 2001, "Evidence of Longitudinal Vortices Evolved from Distorted Wakes in Turbine Passage," *J. Fluid Mech.*, **446**, pp. 199–228.
- [30] Spalart, P.R., Strelets, M.K.H., 2000, "Mechanism of transition and heat transfer in a separation bubble," *J. Fluid Mech.*, Vol. **403**, pp. 329–349.
- [31] Horton, H.P. 1968, "A Semi-Emperical Theory for Growth and Bursting of Laminar Separation Bubbles," PhD Dissertation, University of London.
- [32] Colburn, A. P. 1933, "A method of correlating forced convection heat transfer data and a comparison with fluid friction," *Trans. Am. Inst. Chem. Engrs.* , **29** , pp. 174-210.
- [33] Wu, X., Jacobs, R. G., Hunt, J. R. C., and Durbin, P. A., 1999, "Simulation of Boundary Layer Transition Induced by Periodically Passing Wakes," *J. Fluid Mech.*, **398**, pp. 109–153.
- [34] Alam, M. & Sandham, N. D., 2000, "Direct numerical simulation of 'short' laminar separation bubbles with turbulent reattachment," *J. Fluid Mech.*, **403**, pp. 223–250.
- [35] Watmuff, J. H., 1999, "Evolution of a Wave Packet Into Vortex Loops in a Laminar Separation Bubble," *J. Fluid Mech.*, **397**, pp. 119–169